Journal of Oceanology and Limnology
Vol. 42, No. 4, pp. 1143-1156, 2024
https://doi.org/10.1007/s00343-023-3155-9

Research Paper

Spatial correlations in time and frequency domains between chlorophyll-*a* concentration and environmental factors in the Bohai Sea*

Wan XU[1], Di MU[2], Zhenteng YANG[1], Dekui YUAN[3, **]

[1] *Department of Mechanics, Tianjin University, Tianjin 300350, China*

[2] *Engineering Research Center of Seawater Utilization of Ministry of Education, School of Chemical Engineering and Technology, Hebei University of Technology, Tianjin 300130, China*

[3] *State Key Laboratory of Hydraulic Engineering Simulation and Safety, Tianjin University, Tianjin 300072, China*

Received Aug. 12, 2023; accepted in principle Sep. 28, 2023; accepted for publication Nov. 4, 2023

Abstract Based on the reconstructed MODIS data and ECMWF reanalysis data from 2003 to 2021, spatial correlations between chlorophyll *a* (Chl *a*) and sea surface temperature (SST), photosynthetically available radiation (PAR), aerosol optical thickness (AOT), and wind speed (WS) in the Bohai Sea were analyzed from the perspective of time domain and frequency domain. Results indicate that the frequency-domain analysis was more conducive to revealing the correlations between Chl *a* and environmental factors. The spatial pattern of time-domain correlations was similar to the isobaths of the Bohai Sea, which was positive in shallow waters and negative in deep waters for SST, PAR, and AOT, and was reversed for WS. Frequency-domain correlations were obtained by performing Fourier Transform and were higher than correlations in time domain. The spatial distributions indicated that the effects of SST and PAR on Chl *a* were greater than AOT and WS in the Bohai Sea. Additionally, cross-spectrum analysis was applied to explore the response relationships. A depth-dependent pattern was shown in correlations and time lags, indicating that the influential mechanism of environmental factors on Chl-*a* concentration is related to seawater depth.

Keyword: chlorophyll *a* (Chl *a*); frequency domain; spatial correlation; Bohai Sea

1 INTRODUCTION

Phytoplankton is the main producer of primary productivity in marine environments, which directly affects the richness and diversity of marine organisms (Boyce et al., 2010). As the main pigment of phytoplankton, chlorophyll *a* (Chl *a*) is one of the most important parameters used to measure the biomass and primary production of phytoplankton, and also considered as an indicator to reflect the state of water eutrophication (Jiang and Zhang, 2018). Exploring the distribution patterns of Chl-*a* concentration can help estimate the phytoplankton biomass and is of great significance to understand the mechanism of marine ecosystems.

Previous studies have indicated that the phytoplankton growth is influenced by a variety of climatic and environmental factors, and the method of correlation analysis has been commonly used to address the correlations between Chl *a* and various factors. Researchers have found that SST has a direct impact on the spatial distribution of Chl-*a* concentration in different marine areas such as the East China Sea, the Black Sea, and the Arabian Sea (Chaturvedi, 2005; Kavak and Karadogan, 2012; Ji et al., 2018). For most oceans, correlation between Chl *a* and wind speed (WS) has been found to be negative in deep waters and positive in shallow waters (Kahru et al., 2010). But in the Yellow Sea and the East China Sea, the correlation is negative in shallow coastal areas and positive in deep open

* Supported by the Key Research and Development Program of 14th Five-year Plan of China (No. 2021YFC3200401-04) and the Major Scientific and Technological Projects of Tianjin (No. 18ZXRHSF00270)

** Corresponding author: dkyuan@tju.edu.cn

areas (Zheng et al., 2012). Moreover, significant correlation existed between aerosol deposition and phytoplankton growth, and the correlation coefficients are variable in different sea areas (Nezlin et al., 2010; Tan et al., 2013). However, correlation analysis techniques do not provide information about synchronization between time series. Therefore, the Cross Correlation Function (CCF) has been applied to study the lags in the correlation between Chl *a* and other factors. In the Persian Gulf, the correlation between Chl *a* and SST is positive without time lag in shallow regions, and is negative with time lags of 3–5 months in deep regions (Moradi and Moradi, 2020). In the waters off Somalia, evidences have suggested that there is a time lag of 8 days between aerosol optical thickness (AOT) and Chl *a* (Shafeeque et al., 2017). In the South Yellow Sea, the concentration of Chl *a* will increase in varying degrees 2–8 days after dust deposition, and the response time will shorten as the amount of deposition increases (Zhang et al., 2020).

The Bohai Sea is a shallow marginal sea of the northwestern Pacific Ocean, surrounded by regions with rapid economic development and connected to the Yellow Sea. Large quantities of fresh water, suspended solids and dissolved nutrients are discharged into the Bohai Sea from 16 rivers, among which the Huanghe (Yellow) River contribute more than half of the total discharges (Ning et al., 2010). The input of abundant nutrients has caused serious eutrophication in the Bohai Sea, and overfishing has apparently destroyed the biodiversity (Liu, 2015). Such a change in ecosystem leads to frequent occurrence of algal blooms in the Bohai Sea, which has aroused widespread attention of scholars on Chl-*a* concentration in this area. Zou et al. (2005) pointed out that Chl *a* in the Bohai Sea increases with the increase of SST in the inshore regions while decreases in the central regions. Guo (2014) reported that Chl *a* will keep increasing after strong winds, reaching the peak value in about 4 days, and the entire process will last for more than 15 days. In addition, increases in precipitation over the Bohai Sea should contribute to the rise of Chl-*a* concentration (Tian et al., 2019; Zhai et al., 2021). And human activity also plays an important role in phytoplankton growth (Zhao et al., 2020).

Although there have been studies on correlations between Chl *a* and various factors in the Bohai Sea, most of them are conducted from time domain. A time series consists of three parts, which are frequency, amplitude, and phase. Correlations among the magnitude of variables are usually what we tend to explore. However, since analysis in time domain takes the three as a whole to analyze, the influence of phase difference cannot be eliminated and the correlation might be estimated incorrectly. Nevertheless, the frequency-domain analysis can present the frequency structure of the time series so that the frequency structures of Chl *a* and environmental factors could be compared and the synchronization between them could be analyzed. Meanwhile the information of amplitude and phase could be extracted separately so that relationships between variables can be expressed more explicitly. Therefore, based on methods of time-domain analysis and frequency-domain analysis, this paper aims to study the correlations between Chl *a* and environmental factors (SST, PAR, AOT and WS) over the Bohai Sea and different regions, so as to reflect their essential characteristics.

2 DATA AND METHOD

2.1 Study area

As the largest inland sea of China, the Bohai Sea (Fig.1) is located at 37°70′N–40°59′N and 117°35′E–122°16′E, which is a semi-enclosed north temperate sea area (Wei et al., 2004). It covers an area of about 78 000 km^2, with an average depth of 18 m and a maximum depth of 86 m. According to geographical location, it can be roughly divided into four parts: the Liaodong Bay, the Bohai Bay, the Laizhou Bay, and the Central Bohai Sea. The Bohai Sea is connected to the Yellow Sea through the narrow channel of the Bohai Strait (Li et al., 2019). This

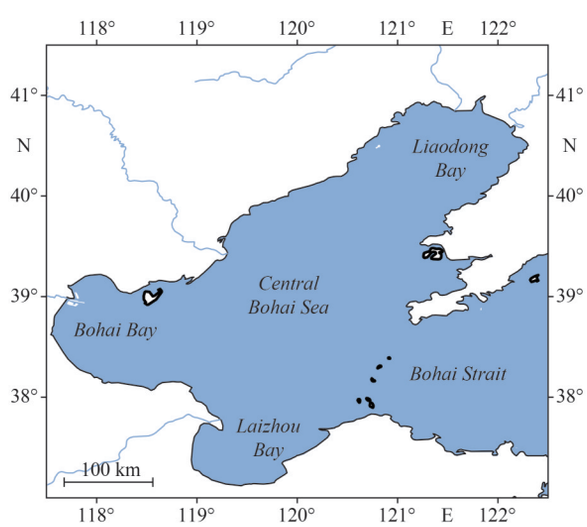

Fig.1 Sketch map of the study area

special geographical condition leads to a long period and a weak capacity of the water exchange between the Bohai Sea and the external sea, which is responsible for the accumulation of nutrients and frequent red tide and green tide events, and its ecosystem is thus seriously threatened (Liu, 2015; Zhou et al., 2017).

2.2 Dataset

The 8-day averaged data of Chl-*a* concentration, SST, PAR, and AOT were derived from MODIS-Aqua Level-3 remotely sensed datasets, downloading from NASA Ocean-Color website (http://oceancolor.gsfc.nasa.gov/) with a spatial resolution of 4 km. The standard Level-3 Chl-*a* product, which was calculated following the (ocean color index) OCI algorithm and the (ocean Chl-*a* three-band algorithm for MODIS) OC3M algorithm, was used in the present study. For WS, ECMWF ERA5 reanalysis data was used in this study, obtaining from the Climate Data Store (https://cds.climate.copernicus.eu/) with a time resolution of an hour and a spatial resolution of 0.25°×0.25°. To produce the same resolutions of MODIS data products, the initial wind speed data were converted into 8-day averaged data by calculation and interpolated into 4 km×4 km gridded data by the inverse distance weighted method. All the data were applied to the study area in the Bohai Sea at 117.25°E–122.50°E and 37°N–41°N, with a period from January 1, 2003 to January 1, 2021. Considering that MODIS data are missing in different degrees, the improved validation-point DINEOF (IV-DINEOF) algorithm was used to interpolate and reconstruct the data before further researches could be carried out (Yang et al., 2023).

Since the satellite remote sensing data can achieve large-scale and long-term observations of global oceans, it has been widely used in the researches of marine ecological environment. In the studies on the Bohai Sea, many researchers chose the MODIS-Aqua remotely sensed data for analysis (Fu et al., 2016; Jiang and Zhang, 2018; Zhao et al., 2020; Zhai et al., 2021). The standard MODIS algorithm is developed for open ocean waters (Case-I waters), of which the sea surface color is mainly determined by chlorophyll (Nezlin, 2008). When this algorithm is used for Case-II waters such as the Bohai Sea, it will overestimate the concentration of Chl *a*. However, since the focus of this study is the trend of the time series rather than the magnitude of the values, the overestimation of the entire series has little or no impact on the results. Therefore, the standard MODIS-Aqua Level-3 datasets could be applied for the following analysis.

2.3 Method

2.3.1 Correlation analysis

The Pearson Correlation Coefficient (PCC) was used to measure the linear correlation between two continuous variables. Assuming that X and Y are two random variables, their correlation coefficient is given as (Pearson, 1920):

$$r=\frac{\sum_{i=1}^{n}\left(x_i-\bar{x}\right)\left(y_i-\bar{y}\right)}{\sqrt{\sum_{i=1}^{n}\left(x_i-\bar{x}\right)^2}\sqrt{\sum_{i=1}^{n}\left(y_i-\bar{y}\right)^2}}, \tag{1}$$

where x_i and y_i are the sample values of X and Y, n is the sample size, $\bar{x}$ and $\bar{y}$ are the mean values of the samples. If r is not equal to zero, a t-test can be applied to test the significance of the correlation between two variables.

In the current study, correlations between two time series were measured by calculating the PCC of them. It should be noticed that frequency-domain analysis used the amplitude series obtained from Fourier Transform to perform correlation calculations.

2.3.2 Fourier Transform

As a common frequency domain analysis method, Fourier Transform can make the transformation of a signal from time domain into frequency domain. Its essence is to decompose the original signal into the superposition of different harmonic components. If f is an integrable function, its Fourier Transform should be expressed as:

$$F(\omega)=\int_{-\infty}^{+\infty}f(t)\mathrm{e}^{-\mathrm{i}\omega t}\,\mathrm{d}t. \tag{2}$$

For the discrete time series $\{x_n\}$ with a length of N, the corresponding Discrete Fourier Transform (DFT) is given as:

$$\begin{aligned}X(k)&=\sum_{n=0}^{N-1}x_n\mathrm{e}^{-\mathrm{i}\frac{2\pi}{N}kn}\\&=\sum_{n=0}^{N-1}x_n\left[\cos\left(\frac{2\pi}{N}kn\right)-\mathrm{i}\sin\left(\frac{2\pi}{N}kn\right)\right]\\&=a(k)-\mathrm{i}b(k),\end{aligned} \tag{3}$$

where $X(k)$ is a complex function, $a(k)$ represents the real part, $b(k)$ represents the imaginary part, and k represents different frequency components. Then the amplitude $A(k)$ and the phase $\varphi(k)$ of the original time series are respectively given as:

$$A(k)=\frac{2\sqrt{a^2(k)+b^2(k)}}{N}, \tag{4}$$

$$\varphi(k)=\arctan\left[-\frac{b(k)}{a(k)}\right]. \tag{5}$$

2.3.3 Cross-spectrum analysis

Cross-spectrum analysis is used to provide information about synchronization between two signals, such as advanced or lagged relationship. The cross-spectral density function can be obtained by applying Fourier transform to the bivariate cross-covariance function, and then the amplitude response and phase relationship will be respectively derived (Yang et al., 2022). The cross-covariance function of two time series $x(t)$ and $y(t)$ is defined as:

$$r_{xy}(k)=\mathrm{cov}\left[x(t),y(t-k)\right], \tag{6}$$

where k refers to the time lag between two series. Then the cross-spectral density function should be expressed as:

$$C_{xy}(\omega)=\sum_{-\infty}^{+\infty}\mathrm{e}^{-\mathrm{i}2\pi\omega k}r_{xy}(k)=P_{xy}(\omega)-\mathrm{i}Q_{xy}(\omega), \tag{7}$$

where ω represents different frequency components.

The cross-spectral density function $C_{xy}(\omega)$ is a complex function, where $P_{xy}(\omega)$ reflects the correlation of in-phase frequency components of two time series, and the imaginary part $Q_{xy}(\omega)$ reflects the correlation of out-phase frequency components. Based on it, the cross-amplitude spectrum $A_{xy}(\omega)$ and the phase spectrum $\varphi_{xy}(\omega)$ can be derived, which are respectively given as:

$$A_{xy}(\omega)=\sqrt{P_{xy}^2(\omega)+Q_{xy}^2(\omega)}, \tag{8}$$

$$\varphi_{xy}(\omega)=\arctan\left[-\frac{Q_{xy}(\omega)}{P_{xy}(\omega)}\right]. \tag{9}$$

For two time series, their response relationship of the frequency components in amplitude can be obtained from Eq.8, and the leading or lagging relationship of them can be obtained from Eq.9.

2.3.4 Mann-Kendall trend test

The Mann-Kendall trend test (MK test) is a non-parametric test used to detect the monotonic trend of a time series (Mallick et al., 2021). In the present study, the MK test was performed to identify the historical trends of Chl *a* and environmental factors in the Bohai Sea. For a long-time series, x_1, x_2, x_3, ⋯, x_n represents n data points. The statistic (S) of the MK test is calculated as follows:

$$S=\sum_{i=1}^{n-1}\sum_{j=i+1}^{n}\mathrm{sgn}\left(x_j-x_i\right), \tag{10}$$

where

$$\mathrm{sgn}\left(x_j-x_i\right)=\begin{cases}1, & x_j-x_i>0\\ 0, & x_j-x_i=0,\\ -1, & x_j-x_i<0\end{cases} \tag{11}$$

when $n\geq 10$, the statistic S is considered to be approximately normal distribution. The mean of S is 0 and the variance (σ^2) of S is given by:

$$\sigma^2=\frac{1}{18}\left[n(n-1)(2n+5)-\sum_{i=1}^{p}t_i(t_i-1)(2t_i+5)\right], \tag{12}$$

where p is the number of groups with the same value in the data set and t_i is the number of data points in the i^{th} tied group. Then the standard normal distribution statistic (Z_{MK}) can be obtained as:

$$Z_{\mathrm{MK}}=\begin{cases}\dfrac{S-1}{\sqrt{\sigma^2}}, & S>0\\ 0, & S=0.\\ \dfrac{S+1}{\sqrt{\sigma^2}}, & S<0\end{cases} \tag{13}$$

The null hypothesis (H_0) shows no trend in the series. At the level of significance α, reject the null hypothesis when $|Z_{\mathrm{MK}}|>Z_{1-\frac{\alpha}{2}}$, which means that the series has significant trend.

2.3.5 Multiple linear regression

Multiple linear regression (MLR) is a statistical technique that uses several explanatory variables to predict the outcome of a response variable. The formula of MLR is given as:

$$Y=\beta_0+\beta_1X_1+\beta_2X_2+\cdots+\beta_nX_n+\varepsilon, \tag{14}$$

where Y is dependent variable, X_1, X_2, ⋯, X_n are independent variables, β_0 is the intercept, β_1, β_2, ⋯, β_n are regression coefficients, and ε is the error term. The coefficient of determination (R^2) of the model is used to measure how much of the variation in dependent variable can be explained by the variations in independent variables. In this paper, the MLR method was applied to study the effect of environmental factors on Chl-*a* concentration. The dependent variable was Chl *a* and the independent variables were SST, PAR, AOT, and WS.

In this research, all the methods mentioned above were applied by programming in Python.

3 RESULT

3.1 Correlation and response relationship over the whole Bohai Sea

3.1.1 The variation characteristics of Chl *a* and environmental factors

As shown in Fig.2, variations of 8-day averaged Chl-*a* concentration and the 4 environmental factors were averaged over the entire Bohai Sea region from 2003 to 2021. The variation of Chl *a* was ranged from 2.63 to 7.21 mg/m^3, and its overall trend was decreasing, which was -0.012 mg/(m^3·a) (Fig.2a). Both SST and PAR had an upward trend during the study period but were not significant, which was 0.089 ℃/a for SST and 0.074 μmol/(m^2·s·a)

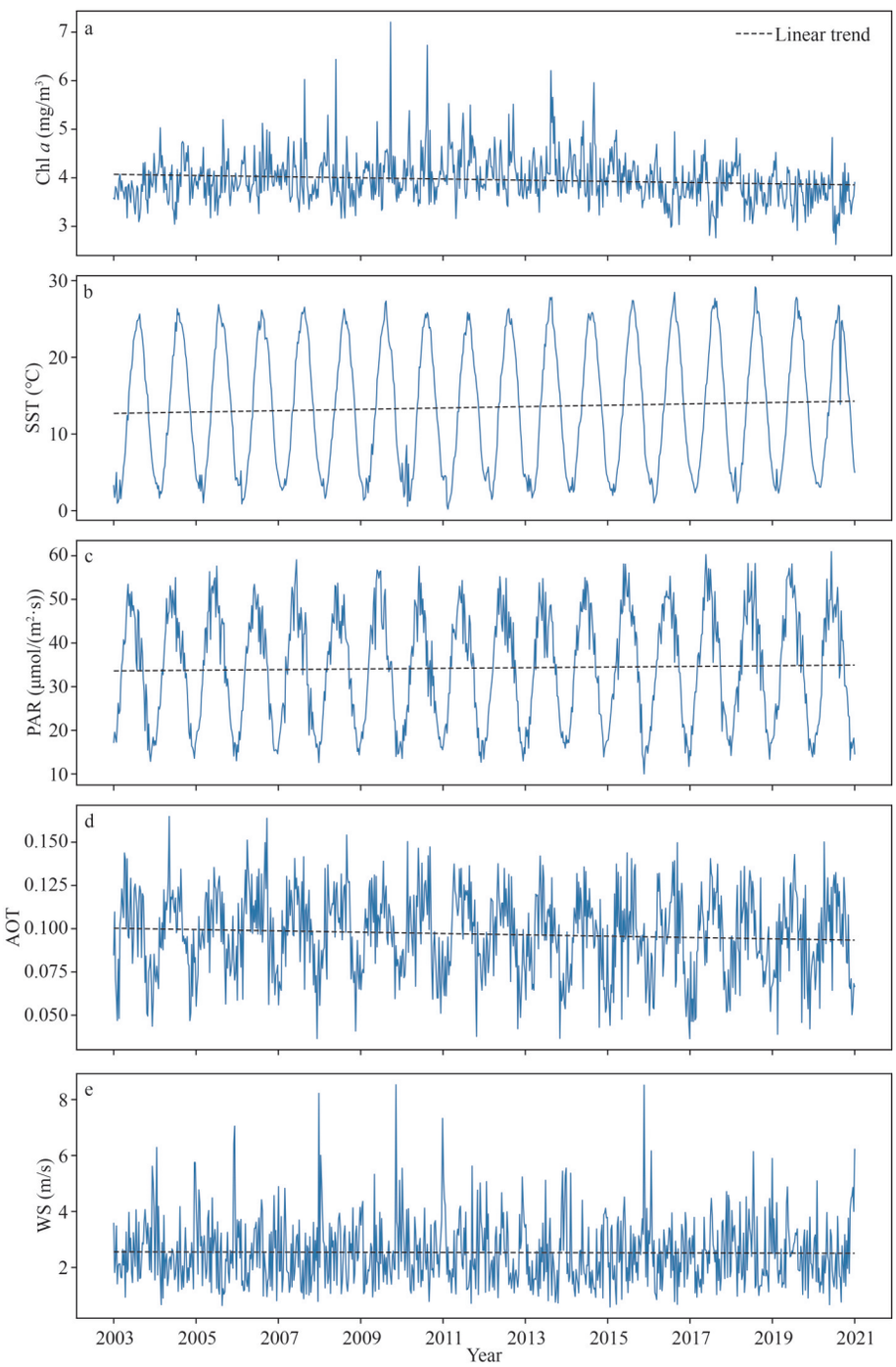

Fig.2 Variations of 8-day averaged valued over the whole Bohai Sea (2003–2021)

for PAR, respectively (Fig.2b & c). The variations of both AOT and WS showed a slow declined trend (Fig.2d & e) and the trend for WS was also insignificant. The rate of decline was -3.83e-4/a for AOT and -0.003 m/(s·a) for WS. To further examine the trend of each time series, the Mann-Kendall test was performed with the confidence level of 95% (Table 1). The results show that Chl *a* and AOT had a significant decreasing trend while the four factors all had no trend, and this is consistent with the above analysis.

Figure 2 demonstrates that the fluctuation of Chl-*a* concentration was obvious while the periodicity was not significant. SST and PAR shared the common periodic characteristics with a period of about 1 year. The periodicity of AOT and WS were less significant, since the fluctuation was stronger than that of SST and PAR. According to their variation characteristics, the patterns of SST and PAR are relatively consistent, thus it can be preliminarily inferred that SST and PAR have a strong correlation.

3.1.2 The frequency characteristic of Chl *a* and environmental factors

Figure 3a displays the frequency spectrum of Chl-*a* concentration during the study period, and shows five high peaks. The peak near the zero-frequency indicated a certain trend of its variation, and for other peaks, their corresponding frequencies were 0.022, 0.043, 0.065, and 0.087, respectively. Based on the correspondence between frequency and period, the frequency of 1.0 represented a period of 8 days in the current study, so the four frequencies corresponded to the peaks, respectively, indicated that variation of Chl *a* had the period of one year, half year, 4 months, and 3 months. Figure 3b–e shows the frequency spectrums of the 4 environmental factors, respectively. The significant peaks at the frequency of 0.022 meant that the fluctuation of environmental factors had a one-year period, which is consistent with the characteristics

Table 1 Mann-Kendall test of Chl *a* and environmental factors from 2003 to 2021 (α=0.05)

Time serie	Trend	*P* value	Z_{MK}	$Z_{(1-\alpha/2)}$	Confidence level
Chl *a*	Decreasing	0.000 3	-3.609	1.960	95%
SST	No trend	0.073 7	1.789	1.960	95%
PAR	No trend	0.386 3	0.866	1.960	95%
AOT	Decreasing	0.028 1	-2.196	1.960	95%
WS	No trend	0.779 9	-0.279	1.960	95%

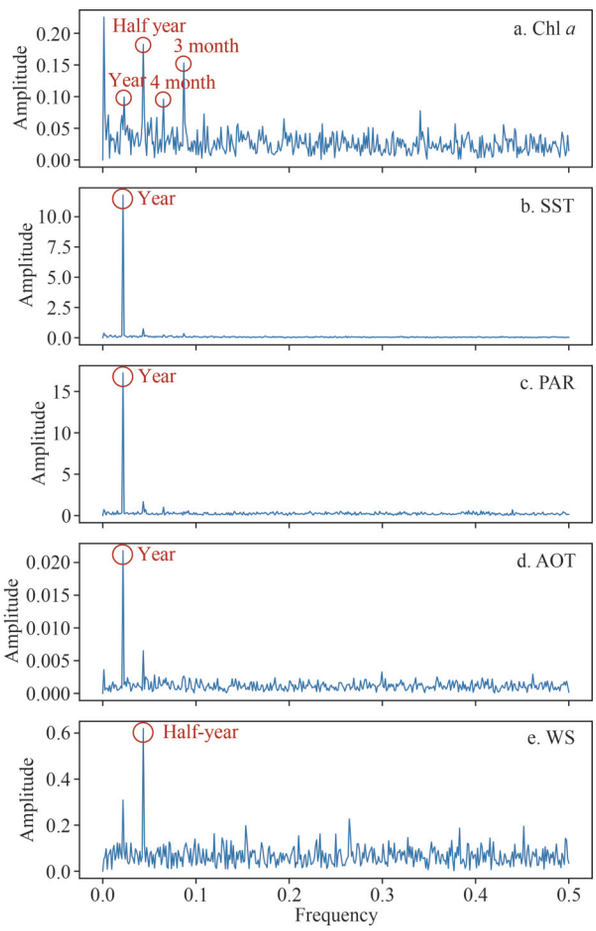

Fig.3 Frequency spectrums of 8-day averaged values over the whole Bohai Sea (2003–2021)

a. Chl *a*; b. SST; c. PAR; d. AOT; e. WS. Periods corresponding to the peaks are marked in the graphs.

reflected in time domain. In addition, WS had a higher peak at the frequency of 0.043, meaning that its half-year period was more significant, which was caused by the climate characteristics of the Bohai Sea. In contrast, the corresponding peaks of SST, PAR and AOT at the same frequency were much lower, indicating that their characteristics of half-year period were not significant.

3.1.3 Correlation between Chl *a* and environmental factors

The Pearson correlation coefficients between Chl-*a* concentration and environmental factors were calculated from the perspective of time domain and frequency domain, respectively (Fig.4). The time-domain correlations were obtained by performing correlation calculations on the time series (Fig.4a), while the frequency-domain correlations were calculated using the Fourier-transformed frequency-amplitude series (Fig.4b).

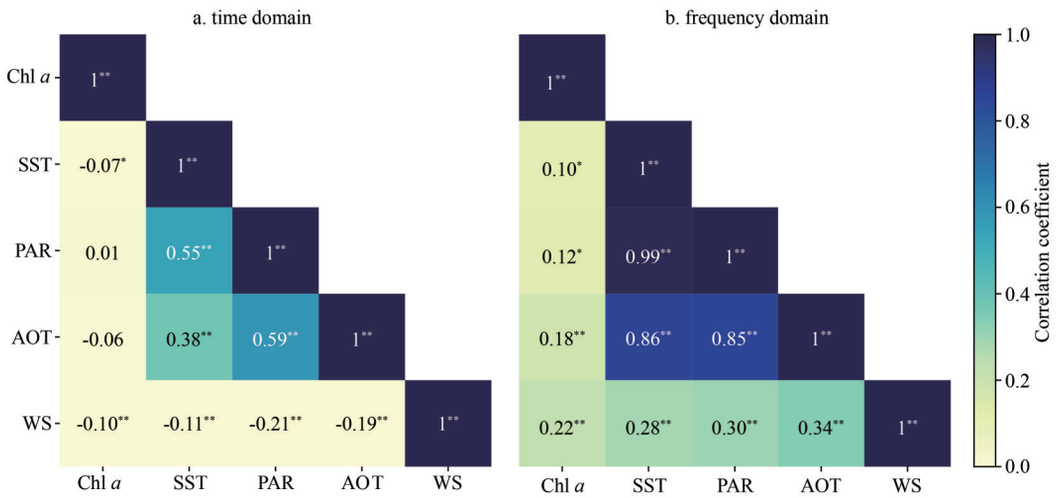

Fig.4 Correlation coefficients of time domain (a) and frequency domain (b) between Chl *a* and environmental factors over the whole Bohai Sea (2003–2021)

The superscript ** means $P<0.01$ while * means $0.01<P<0.05$.

As shown in Fig.4a, in time domain, correlations between Chl *a* and PAR and AOT were not statistically significant, while other factors were all weakly correlated with Chl-*a* concentration in the Bohai Sea, which has also been reported in other studies (Tian et al., 2019). In addition, there should be a strong correlation between SST and PAR according to the analysis above, but the value of it was only 0.55. This should be attributed to the influence of phase difference which could not be eliminated in time domain and resulted in incomplete reflected correlations between variables. Therefore, it is necessary to conduct correlation analysis from the perspective of frequency domain (Fig.4b). Obviously, correlation coefficients among the amplitude series of the variables were improved significantly. The coefficient between SST and PAR reached 0.99, indicating that their responses at various frequencies were almost identical. The correlations between Chl *a* and environmental factors were all statistically significant although they were still not strong. The weak correlations should be due to the averaging of the whole area, which led to the spatial analysis in following discussions (Section 3.2).

3.1.4 Response relationship between Chl *a* and environmental factors

Aiming to obtain the time lags between Chl-*a* concentration and environmental factors in the Bohai Sea, the cross-spectrum analysis was applied to explore their response relationships from frequency domain (Fig.5).

The left panel of Fig.5 gives the cross-amplitude spectrums between Chl *a* and each environmental factor respectively, and the cross-amplitude spectrums between SST and PAR, and their corresponding phase spectrums were shown in the right panel. It can be seen that the frequency corresponding to the maximum amplitude was 0.022 for SST and PAR (Fig.5a & c), and 0.043 for AOT and WS (Fig.5e & g). This indicates that Chl *a* had the most significant response to SST and PAR under one-year period, and to AOT and WS under half-year period. The phase corresponding to the frequency refers to the phase difference between Chl *a* and each factor, which was 1.997 rad, 2.895 rad, 0.086 rad, and 3.001 rad (Fig.5b, d, f, & h, respectively). The results suggest that SST and PAR were respectively ahead of the variation of Chl *a* by 117.0 days and 169.6 days under the one-year period, while AOT and WS were respectively 2.5 days and 87.9 days ahead of Chl *a* under the half-year period. According to the correlation coefficients (Fig.4) and the response relationships, AOT was positively correlated with Chl-*a* concentration and their variations were almost synchronous, illustrating that AOT may directly promote the growth and reproduction of phytoplankton. In addition, the response between SST and PAR was strongest under the one-year period, and SST lagged behind PAR by 56.7 days (Fig.5i & j). This is consistent with the common sense and can be verified from their temporal variations (Fig.3b & c), indicating the rationality of the cross-spectrum analysis.

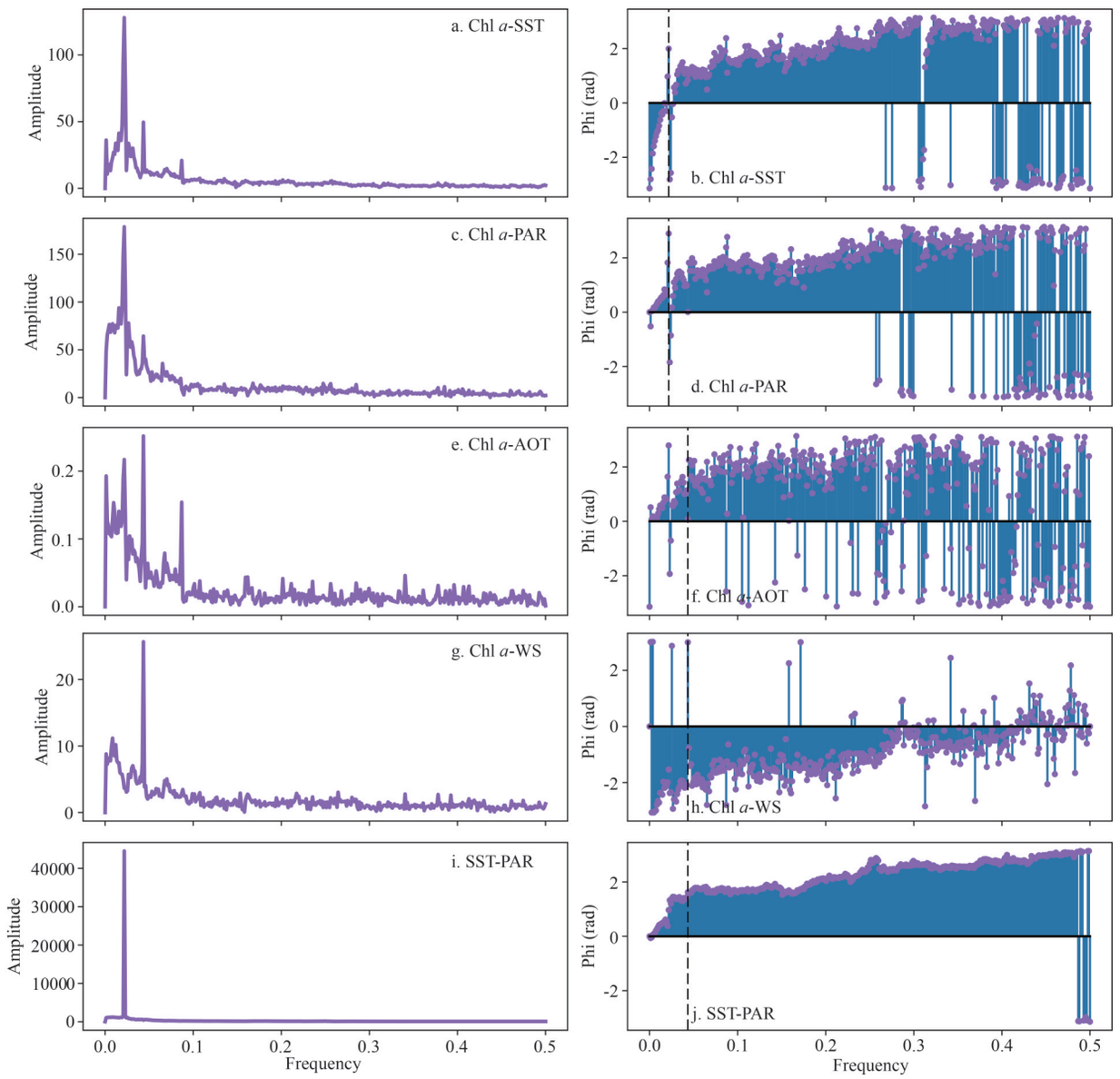

Fig.5 Cross-amplitude spectrums (left panel) and phase spectrums (right panel) between Chl *a* and SST (a and b), Chl *a* and PAR (c and d), Chl *a* and AOT (e and f), Chl *a* and WS (g and h), and SST and PAR (i and j) over the whole Bohai Sea (2003–2021)

3.2 Correlation and response relationship in different regions of the Bohai Sea

3.2.1 Spatial characteristic of correlations

Having conducted an analysis of the averaged data over the whole Bohai Sea, correlations and response relationships in different regions were further studied. Spatial correlations between Chl *a* and environmental factors were calculated from time domain and frequency domain as demonstrate in Figs.6 & 7, respectively. In addition, the bathymetric chart of the Bohai Sea is shown in Fig.8 for the convenience of analysis on the spatial characteristics.

From the spatial distributions of time-domain correlations (Fig.6), it can be found that correlation coefficients between Chl *a* and the four factors are similar in pattern to the isobaths of the Bohai Sea (Fig.8). This pattern had two distinct regions, positive shallower waters and negative deeper waters for SST, PAR, and AOT, and the pattern was reversed for WS. By comparison, the time-domain correlation between Chl *a* and SST was relatively stronger, and its absolute value reached around 0.5. And the correlation between Chl *a* and WS was relatively weaker, and varied in the range of -0.2–0.2. The

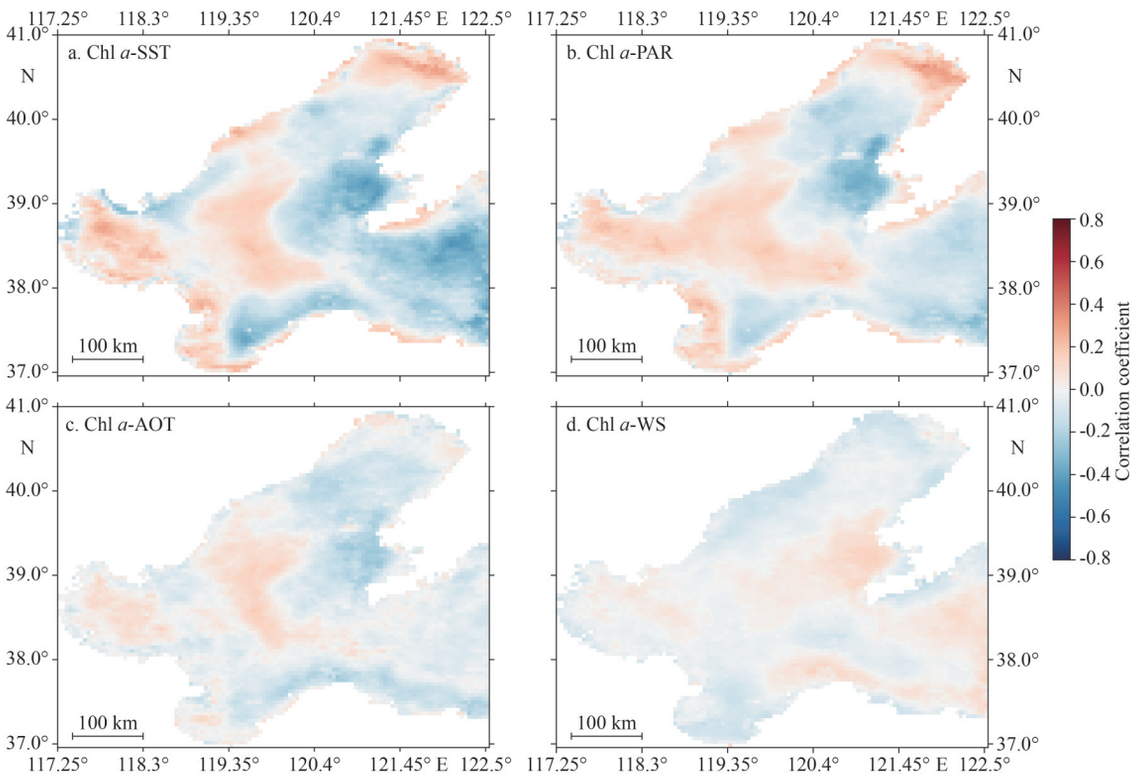

Fig.6 Spatial distributions of time-domain correlations between Chl *a* and SST (a), PAR (b), AOT (c), and WS (d) in the Bohai Sea (2003–2021)

The color shades represent the value of correlation coefficient, which is in the range of -0.8–0.8. Statistical correlations were calculated under confidence level 95%.

result of spatial analysis is quite different from that shown in Fig.4a, indicating that averaging the whole area may lose the characteristics of local areas.

In frequency domain, the correlation coefficients between Chl *a* and environmental factors all increased and could reach around 0.8 (Fig.7). It is noteworthy that the distribution patterns of SST and PAR appeared largely the same. The correlation coefficients between Chl *a* and these two factors were higher in eastern deep regions and lower in western shallow regions. As for the correlation between Chl *a* and AOT and WS, their spatial distributions were relatively uniform. Although they were also stronger in eastern Bohai Sea, the overall difference was unobvious. Besides, sudden changes may occur at some points along the coast (Fig.7c), which may be related to the deficiency of data itself, thus it was not considered in this discussion. Overall, the frequency-domain correlations between Chl *a* and AOT and WS were relatively weaker compared with SST and PAR, indicating that the effects of SST and PAR on the concentration of Chl *a* were greater than the other two factors.

3.2.2 Spatial characteristic of response relationships

The spatial distributions of response relationships were obtained by cross spectrum analysis as presented in Figs.9 & 10.

Figure 9 gives the spatial distributions of the periods corresponding to the strongest response between Chl *a* and the factors. It can be seen that only WS followed a biannual period in western regions and an annual period in most eastern regions, while the other factors all presented an annual period over the Bohai Sea. Under the period of one year, time lags between Chl *a* and environmental factors had significant spatial characteristics (Fig.10). In coastal regions of the Bohai Sea, SST almost varied synchronously with Chl *a* while PAR and AOT were ahead of Chl *a*. In central and eastern deeper regions, the three factors all lagged behind the variation of Chl *a*, which seemed to be unreasonable. Actually, under the period of one year, the lag of less than half a year can be regarded as the lead of more than half a year. And the cross-spectrum analysis always presents the shorter one as the result. From this point of view,

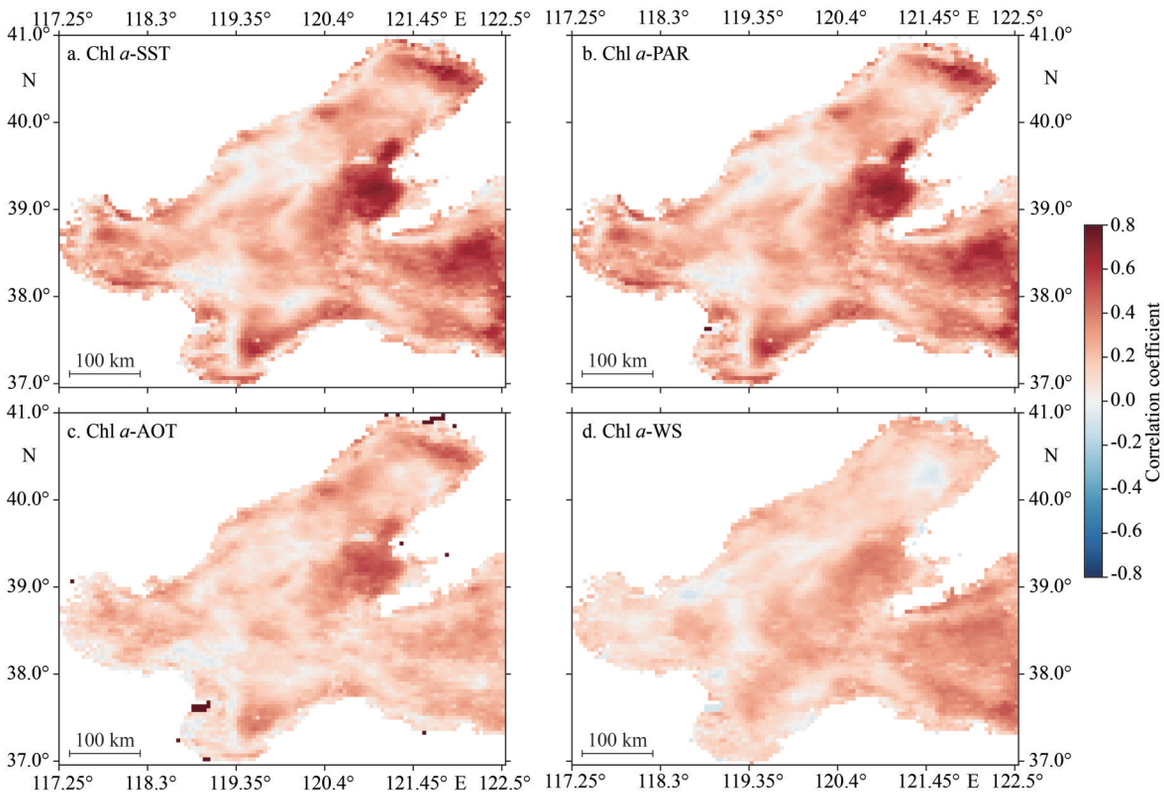

Fig.7 Spatial distributions of frequency-domain correlations between Chl *a* and SST (a), PAR (b), AOT (c), and WS (d) in the Bohai Sea (2003–2021)

The color shades represent the value of correlation coefficient, which is in the range of -0.8–0.8. Statistical correlations were calculated under confidence level 95%.

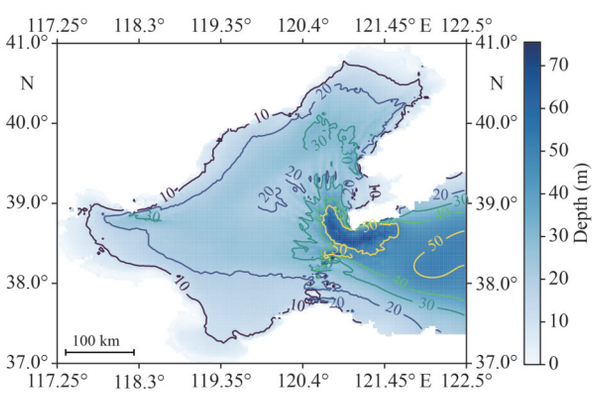

Fig.8 Bathymetric chart of the Bohai Sea with the depth of 10, 20, 30, and 50 m

SST, PAR, and AOT were ahead of Chl *a* for a longer time in deeper waters. In addition, the response period between Chl *a* and WS varied from half a year to one year as the depth increased, illustrating that the response relationship is related to the sea depth.

4 DISCUSSION

Previous researches have reported that concentration of Chl *a* is positively correlated with SST in shallow regions, while there is a negative correlation in deep regions (Shen et al., 2008; Jutla et al., 2011; Moradi and Moradi, 2020). Results of this study verified the previous conclusions. In shallow waters, nutrients and temperature are the main controlling factors of phytoplankton growth (Moradi and Moradi, 2020). Since terrestrial inputs bring abundant nutrients into coastal waters, a relatively high correlation of frequency domain with a near-zero time lag between Chl *a* and SST was observed in this area. In deep waters, the rise in SST should result in a seasonal thermocline, blocking the nutrients supplement from the bottom to the surface. The thermocline will gradually disappear as SST decreases, and surficial nutrients will be enriched, promoting the growth of phytoplankton. Consequently, the frequency response of Chl *a* was highly correlated with that of SST in deep regions in magnitude. And the time lag of about half a year shows the seasonal characteristics of SST. In time domain, this close relationship was presented by a significant negative correlation between them.

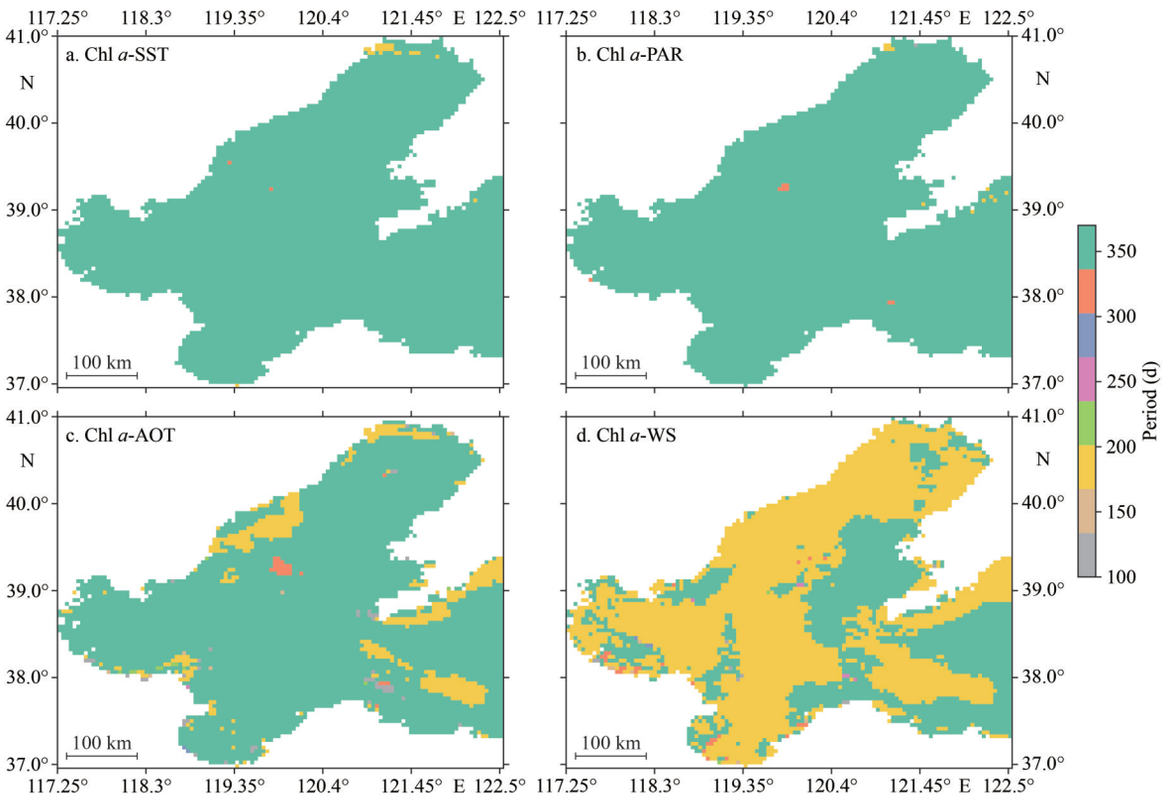

Fig.9 Spatial distributions of the periods corresponding to the strongest response between Chl *a* and SST (a), PAR (b), AOT (c), and WS (d) in the Bohai Sea (2003–2021)

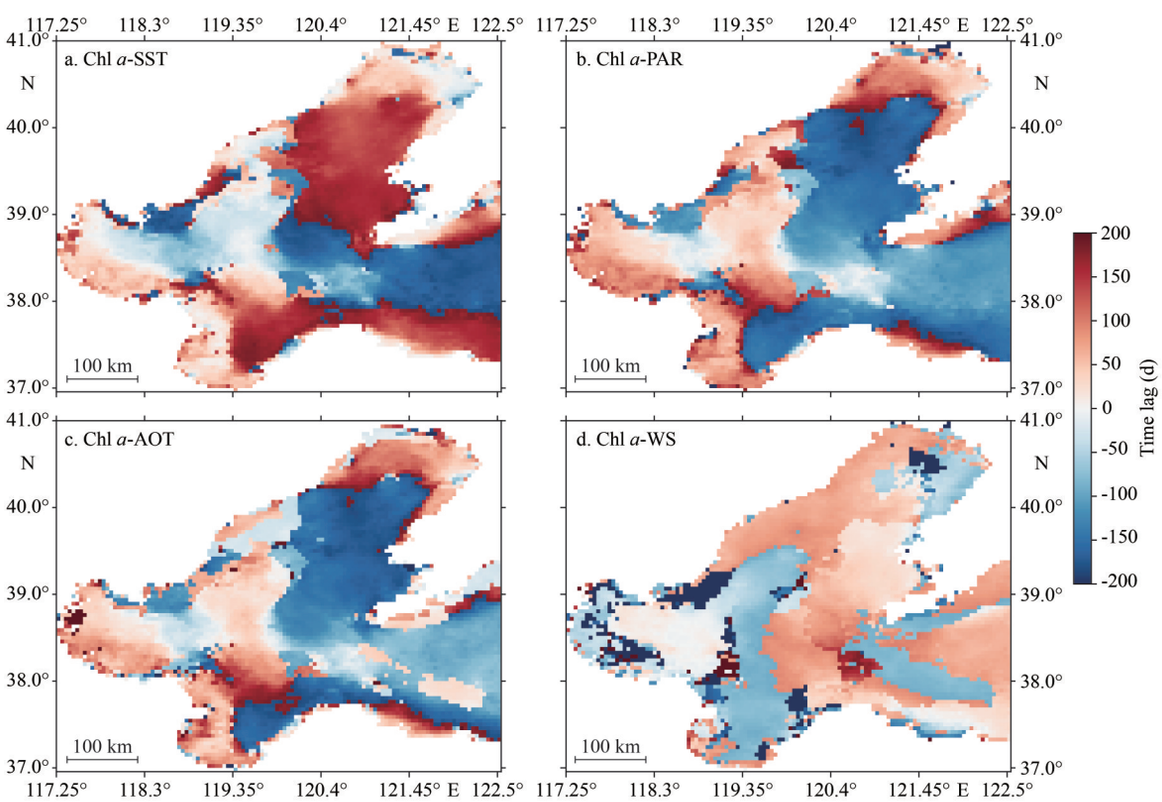

Fig.10 Spatial distributions of time lags between Chl *a* and SST (a), PAR (b), AOT (c), and WS (d) under the corresponding period in the Bohai Sea (2003–2021)

Photosynthesis of phytoplankton directly depends on light and nutrients, so Chl *a* and PAR are likely to show a significant causal relationship. Here, the pattern of time-domain correlation between Chl *a* and PAR is similar to that between Chl *a* and SST, and their frequency-domain correlations almost coincide. It can be inferred that solar radiation has a direct impact on the temperature of sea surface, which was also shown in the high similarity between SST and PAR in frequency structure. Since SST always lags behind the variation of PAR, the time lag between Chl *a* and PAR is longer than that between Chl *a* and SST. And the time lag of more than half a year in deeper regions will result in a lower correlation in time domain.

In the study on the Persian Gulf, Moradi and Moradi (2020) found that Chl *a* was positively correlated with AOT with a time lag of 1–3 months. In this paper, the same result could be observed in shallowest waters of the Bohai Sea. The aerosol deposition is considered as the fertilizer for phytoplankton growth, since it contains the essential nutrients (Kotta and Kitsiou, 2019). However, a weak negative correlation was found in deeper regions, which should be related to the longer time lag between Chl *a* and AOT. Due to the lower wind speed, AOT reaches its maximum value in summer, during which the thermocline forms in deep waters with the increase of SST. Therefore, in deeper regions, the increasing AOT cannot lead to an immediate increase in Chl *a* but with a time lag of more than half a year.

Wind also has a great influence on the distribution of phytoplankton on the ocean surface. As an effective factor controlling upwelling and vertical mixing, wind directly affects the depth of the mixed layers. Kahru et al. (2010) pointed out that the high-positive correlation between Chl-*a* concentration and WS occurred in the area with relatively shallow mixed layers, where it was easier for winds to deepen the mixed layers and bring nutrients into the upper layers. In this paper, the mixed layers are relatively shallow on the whole since the average depth of the Bohai Sea is only 18 m. However, a positive correlation between WS and Chl *a* only appeared in most deeper regions, where the growth of phytoplankton was mainly limited by surficial nutrients. In coastal waters, the surficial nutrients are abundant due to terrestrial inputs, and the mixed layers are too shallow. The strong winds will shorten the survival of phytoplankton in euphotic layer, resulting in a weak negative correlation in coastal regions.

To sum up, light conditions, temperature, and vertical stability of seawater in many temperate sea areas have obvious seasonal cycles, as shown in this paper. Their combined effects lead to significant periodic characteristics of Chl *a* in the Bohai Sea, mainly in the form of double peaks in spring and autumn (Fei et al., 1988). In addition, the effect of atmospheric pollution sources represented by aerosols should also be considered. Compared to time domain, analysis in frequency domain could provide more explanation for the relationships between Chl *a* and these factors. Frequency-domain correlations indicated that the impact of SST and PAR on Chl *a* appeared to be more significant compared with AOT and WS. Cross-spectrum analysis illustrated that the negative correlations could be attributed to the time lags between them, as mentioned before.

Moreover, spatial analysis showed a depth-dependent pattern over the Bohai Sea, meaning that the correlations and response relationships should be related to depth. However, Zoljoodi et al. (2022) pointed that the phenological metrics were not simply related to bathymetry. Therefore, the multiple linear regression was performed in each zone of 4 km×4 km, with Chl *a* as dependent variable and environmental factors as independent variables. The spatial distribution of R^2 is presented in Fig.11. It could be found that R^2 is greater in deep regions, indicating that variations in environmental factors could give more explanation for the variation in Chl *a* in deep waters. This is reasonable since Chl *a* in shallow regions could be affected by more factors, such as terrestrial inputs and human

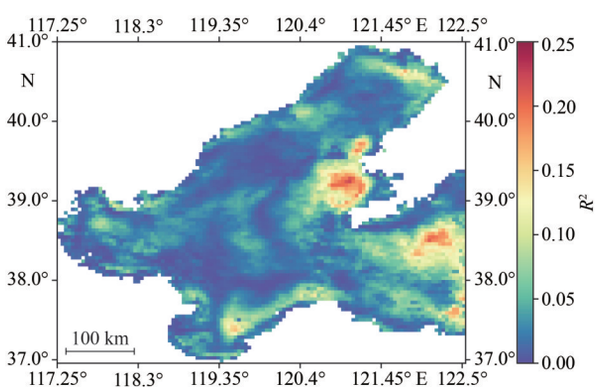

Fig.11 Spatial distribution of the coefficient of determination (R^2) of the multiple linear regression model

activities. The impact of depth on correlations between Chl *a* and environmental factors should be reflected by more parameters, which needs to be explored in further researches.

5 CONCLUSION

Spatial correlations between Chl-*a* concentration and environmental factors (SST, PAR, AOT, and WS) in the Bohai Sea from 2003 to 2021 were analyzed from the perspective of time domain and frequency domain respectively, based on the reconstructed MODIS Level-3 data and ECMWF reanalysis data. The methods of Fourier Transform and cross-spectrum analysis were applied and some conclusions have been derived.

In time domain, the spatial pattern of correlations between Chl *a* and the factors was coincident with bathymetric contour of the Bohai Sea. It was positive in shallow waters and negative in deep waters for SST, PAR, and AOT, while it was reversed for WS.

Frequency-domain correlations were higher than time-domain and also presented a depth-dependent pattern. Since the frequency structure reflects the essential characteristics of time series, the frequency-domain correlations should be more credible. Their distributions showed that the effects of SST and PAR on Chl *a* appeared to be greater than AOT and WS in the Bohai Sea. Cross-spectrum analysis was performed to obtain the time lags that are increased as the sea water deepened and could be an explanation for negative correlations.

Obvious differences in the correlations and time lags are shown between deep waters and shallow waters, indicating that the influential mechanism of environmental factors is related to water depth. Furthermore, the result of MLR shows that variations of the four environmental factors could give more explanation for the variation of Chl *a* in deep waters. More parameters need to be considered in follow-up studies to explain this depth-dependent pattern.

6 DATA AVAILABILITY STATEMENT

The data presented in this article are publicly available in NASA Ocean-Color website at http://oceancolor.gsfc.nasa.gov/, and in the Climate Data Store at https://cds.climate.copernicus.eu/.

7 ACKNOWLEDGMENT

We appreciate NASA for providing the MODIS data and the European Centre for Medium-Range Weather Forecasts for providing the ERA5 data.

References

Boyce D G, Lewis M R, Worm B. 2010. Global phytoplankton decline over the past century. *Nature*, **466**(7306): 591-596, https://doi.org/10.1038/nature09268.

Chaturvedi N. 2005. Variability of chlorophyll concentration in the Arabian Sea and Bay of Bengal as observed from SeaWiFS data from 1997-2000 and its interrelationship with sea surface temperature (SST) derived from NOAA AVHRR. *International Journal of Remote Sensing*, **26**(17): 3695-3706, https://doi.org/10.1080/01431160500159818.

Fei Z L, Mao X H, Zhu M Y et al. 1988. Study on productivity of the Bohai Sea: distribution characteristics and seasonal variation of chlorophyll-*a*. *Acta Oceanologica Sinica*, **10**(1): 99-106. (in Chinese)

Fu Y Z, Xu S G, Liu J W. 2016. Temporal-spatial variations and developing trends of Chlorophyll-*a* in the Bohai Sea, China. *Estuarine*, *Coastal and Shelf Science*, **173**: 49-56, http://doi.org/10.1016/j.ecss.2016.02.016.

Guo J R. 2014. The Method Study of Remote Sensing Data Reconstruction and Its Application in Multi-Scale Variations of Chlorophyll in East China Sea. Ocean University of China, Qingdao, China. (in Chinese with English abstract)

Ji C X, Zhang Y Z, Cheng Q M et al. 2018. Evaluating the impact of sea surface temperature (SST) on spatial distribution of chlorophyll-*a* concentration in the East China Sea. *International Journal of Applied Earth Observation and Geoinformation*, **68**: 252-261, https://doi.org/10.1016/j.jag.2018.01.020.

Jiang D J, Zhang H. 2018. Analysis of spatial and temporal characteristics of chlorophyll-*a* concentration and red tide monitoring in Bohai Sea. *Marine Sciences*, **42**(5): 23-31, http://doi.org/10.11759/hykx20171215001. (in Chinese with English abstract)

Jutla A S, Akanda A S, Griffiths J K et al. 2011. Warming oceans, phytoplankton, and river discharge: implications for cholera outbreaks. *The American Journal of Tropical Medicine and Hygiene*, **85**(2): 303-308, https://doi.org/10.4269/ajtmh.2011.11-0181.

Kahru M, Gille S T, Murtugudde R et al. 2010. Global correlations between winds and ocean chlorophyll. *Journal of Geophysical Research*: *Oceans*, **115**(C12): C12040, https://doi.org/10.1029/2010JC006500.

Kavak M T, Karadogan S. 2012. The relationship between sea surface temperature and chlorophyll concentration of phytoplanktons in the Black Sea using remote sensing techniques. *Journal of Environmental Biology*, **33**(2 Suppl): 493-498.

Kotta D, Kitsiou D. 2019. Exploring possible influence of dust episodes on surface marine chlorophyll concentrations. *Journal of Marine Science and Engineering*, **7**(2): 50, https://doi.org/10.3390/jmse7020050.

Li Y Y, Feng H, Yuan D K et al. 2019. Mechanism study of transport and distributions of trace metals in the Bohai

Bay, China. *China Ocean Engineering*, **33**(1): 73-85, https://doi.org/10.1007/s13344-019-0008-6.

Liu S M. 2015. Response of nutrient transports to water-sediment regulation events in the Huanghe basin and its impact on the biogeochemistry of the Bohai. *Journal of Marine Systems*, **141**: 59-70, https://doi.org/10.1016/j.jmarsys.2014.08.008.

Mallick J, Talukdar S, Alsubih M et al. 2021. Analysing the trend of rainfall in Asir region of Saudi Arabia using the family of Mann-Kendall tests, innovative trend analysis, and detrended fluctuation analysis. *Theoretical and Applied Climatology*, **143**(1): 823-841, https://doi.org/10.1007/s00704-020-03448-1.

Moradi M, Moradi N. 2020. Correlation between concentrations of chlorophyll-*a* and satellite derived climatic factors in the Persian Gulf. *Marine Pollution Bulletin*, **161**: 111728, https://doi.org/10.1016/j.marpolbul.2020.111728.

Nezlin N P. 2008. Seasonal and interannual variability of remotely sensed chlorophyll. *In*: Kostianoy A G, Kosarev A N eds. The Black Sea Environment. Springer, Berlin, Heidelberg. p.333-349, https://doi.org/10.1007/698_5_063.

Nezlin N P, Polikarpov I G, Al-Yamani F Y et al. 2010. Satellite monitoring of climatic factors regulating phytoplankton variability in the Arabian (Persian) Gulf. *Journal of Marine Systems*, **82**(1-2): 47-60, https://doi.org/10.1016/j.jmarsys.2010.03.003.

Ning X R, Lin C L, Su J L et al. 2010. Long-term environmental changes and the responses of the ecosystems in the Bohai Sea during 1960-1996. *Deep Sea Research Part II*: *Topical Studies in Oceanography*, **57**(11-12): 1079-1091, https://doi.org/10.1016/j.dsr2.2010.02.010.

Pearson K. 1920. Notes on the history of correlation. *Biometrika*, **13**(1): 25-45, https://doi.org/10.2307/2331722.

Shafeeque M, Sathyendranath S, George G et al. 2017. Comparison of seasonal cycles of phytoplankton chlorophyll, aerosols, winds and sea-surface temperature off Somalia. *Frontiers in Marine Science*, **4**: 386, https://doi.org/10.3389/fmars.2017.00386.

Shen S, Leptoukh G G, Acker J G et al. 2008. Seasonal variations of chlorophyll *a* concentration in the northern South China Sea. *IEEE Geoscience and Remote Sensing Letters*, **5**(2): 315-319, https://doi.org/10.1109/LGRS.2008.915932.

Tan S C, Yao X H, Gao H W et al. 2013. Variability in the correlation between Asian dust storms and chlorophyll a concentration from the north to equatorial Pacific. *PLoS One*, **8**(2): e57656, https://doi.org/10.1371/journal.pone.0057656.

Tian H Z, Liu Q P, Goes J I et al. 2019. Temporal and spatial changes in chlorophyll *a* concentrations in the Bohai Sea in the past two decades. *Haiyang Xuebao*, **41**(8): 131-140, https://doi.org/10.3969/j.issn.0253-4193.2019.08.013. (in Chinese with English abstract)

Wei H, Sun J, Moll A et al. 2004. Phytoplankton dynamics in the Bohai Sea—observations and modelling. *Journal of Marine Systems*, **44**(3-4): 233-251, https://doi.org/10.1016/j.jmarsys.2003.09.012.

Yang J, Li W T, Zhang Y F. 2022. An empirical study on China's economic cycle and financial cycle based on cross spectrum analysis. *Journal of SUIBE*, **29**(3): 25-39, https://doi.org/10.16060/j.cnki.issn2095-8072.2022.03.002. (in Chinese with English abstract)

Yang Z T, Xia X C, Teo F Y et al. 2023. An improved DINEOF algorithm based on optimized validation points selection method. *Water*, **15**(3): 392, https://doi.org/10.3390/w15030392.

Zhai F G, Wu W F, Gu Y Z et al. 2021. Interannual-decadal variation in satellite-derived surface chlorophyll-*a* concentration in the Bohai Sea over the past 16 years. *Journal of Marine Systems*, **215**: 103496, https://doi.org/10.1016/j.jmarsys.2020.103496.

Zhang L Y, Wang W C, Luo C H et al. 2020. Effects of dust transport path and deposition on chlorophyll *a* concentration in the South Yellow Sea. *Periodical of Ocean University of China*, **50**(8): 9-18, https://doi.org/10.16441/j.cnki.hdxb.20190423. (in Chinese with English abstract)

Zhao N, Wang X P, Li Y S et al. 2020. Temporal-spatial distribution of chlorophyll-*a* and impacts of environmental factors in the Bohai Sea and Yellow Sea. *Science Technology and Engineering*, **20**(17): 7101-7107, https://doi.org/10.3969/j.issn.1671-1815.2020.17.058. (in Chinese with English abstract)

Zheng X S, Wei H, Wang Y H. 2012. Seasonal and interannual variations of chlorophyll-*a* concentration based on the remote sensing data in the Yellow Sea and East China Sea. *Oceanologia et Limnologia Sinica*, **43**(3): 649-654. (in Chinese with English abstract)

Zhou Y L, Zhang C S, Shi X Y et al. 2017. Distribution characteristics of chlorophyll a and its influencing environmental factors in Bohai Sea and Yellow Sea. *China Environmental Science*, **37**(11): 4259-4265, https://doi.org/10.3969/j.issn.1000-6923.2017.11.031. (in Chinese with English abstract)

Zoljoodi M, Moradi M, Moradi N. 2022. Seasonal and interannual cycles of total phytoplankton phenology metrics in the Persian Gulf using ocean color remote sensing. *Continental Shelf Research*, **237**: 104685, https://doi.org/10.1016/j.csr.2022.104685.

Zou B, Zou Y R, Jin Z G. 2005. Analysis of characteristics of seasonal and spatial variations of SST and chlorophyll concentration in the Bohai Sea. *Advances in Marine Science*, **23**(4): 487-492, https://doi.org/10.3969/j.issn.1671-6647.2005.04.015. (in Chinese with English abstract)